JET–P(91)02

J.A. Wesson
and JET Team

Non-Linear Behaviour in Tokamaks

Non-Linear Behaviour in Tokamaks

J.A. Wesson
and JET Team*

JET-Joint Undertaking, Culham Science Centre, OX14 3DB, Abingdon, UK

** See Appendix 1*

Summary of Invited Lecture at the International Toki Conference on
Non-Linear Phenomena in Fusion Plasmas

Non-linear Behaviour in Tokamaks

J.A. Wesson

JET Joint Undertaking
Abingdon, Oxfordshire, England

The range of non-linear phenomena observed in tokamaks is extensive. Rather than summarise their behaviour, it is perhaps more interesting to choose specific subjects which present clearly identifiable theoretical problems. We shall look at three such cases:

i) Fast instabilities

ii) The sequence of events in disruptions

iii) Sawtooth reconnection

The problem of fast instabilities is widely misunderstood. It is generally assumed that the experimental observation of a fast growing instability can be understood if an appropriate mode with a fast growth rate can be found. As we shall see in the next section, this is not so.

In the early days of tokamak research it was common to hear the question - "What is the cause of disruptions?" It is now recognised that a disruption is usually a complex sequence of events posing several theoretical questions. We shall find possible explanations for some of the events, but still be left with a problem regarding the energy quench phase.

When sawtooth oscillations were first observed it was immediately apparent that the relaxation phase occurred on much too short a timescale for simple resistive rearrangement of the magnetic flux to occur. Kadomtsev suggested that the timescale could be understood if the reconnection takes place in a narrow layer at the $q = 1$ surface. It turned out that Kadomtsev's proposed model is indeed the solution of the resistive mhd equations for an $m=1$ instability. However, for large tokamaks at least, the observed sawtooth collapse time is an order of magnitude shorter than predicted by Kadomtsev's model. In the third section the reconnection process is re-examined and a new model with an order of magnitude faster reconnection is described.

i) Fast Instabilities

The procedure in linear stability calculations is to take an equilibrium solution of the equations and, assuming that perturbations have a time dependence $e^{\gamma t}$, to calculate the growth rate γ. A fast instability is then associated with a strongly unstable equilibrium.

It is clear that in most cases of interest this does not represent the actual behaviour. In tokamaks it is not possible to produce strongly unstable axisymmetric equilibria because the timescales required for equilibrium development are much longer than the timescale of fast instabilities.

We can attempt a quantitative description by using the approximation for the perturbation

$$\xi = \xi_o \exp \int_o^t \gamma(t)\,dt$$

where marginal stability is passed at a time taken to be t=0 and the perturbation at that time is ξ_o. Taking as a simple example $\gamma = \dot{\gamma} t$ we obtain

$$\gamma^2 = 2\dot{\gamma}\, \ell n \frac{\xi}{\xi_o}$$

Now if ξ is first observed at a level ξ_{obs} and if the growth rate is then γ_{obs}, we can write

$$\gamma_{obs} = \frac{1}{\tau_{eq}}\, 2\, \ell n \frac{\xi_{obs}}{\xi_o} \qquad (1)$$

where $\tau_{eq} (= \gamma_{obs} / \dot{\gamma})$ is the time taken for the changing equilibrium to produce a growth rate γ_{obs}.

Equation (1) makes the problem clear. The observed growth time is a few times less than a characteristic equilibrium time and this would seem to preclude the appearance of fast instabilities.

The problem can be made even clearer by considering a particular case and the sawtooth collapse on JET provides a carefully investigated example. Figure 1 shows the measured displacement of the peak of the soft X-ray radiation profile for three sawteeth. The displacement appears out of the noise level at ~ 1 cm and then increases to ~ 50 cms with a characteristic growth time of 25 μs.

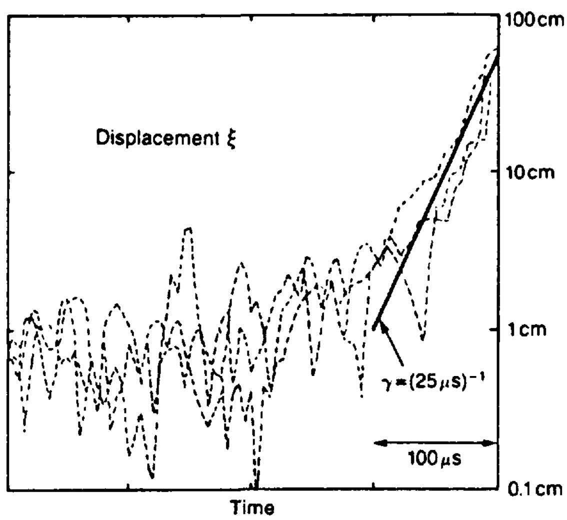

Figure 1 Graphs of the magnitude of the displacement, ξ, of the peak X-ray emission for three sawtooth collapses taken from different discharges. The initial noise level is ~ 1 cm and the growth rises out of this noise with a growth rate ~ (25 μs)$^{-1}$, increasing the displacement to ~ 50 cms in ~ 100 μs.

The expected behaviour depends somewhat on the particular instability imagined to underlie the behaviour, but the essential result does not depend on the instability. In all cases the time which would be taken for the equilibrium to evolve from marginal stability to the observed growth rate is $\gtrsim$ 100 ms. Thus on a millisecond timescale the growth rate does not change. We should therefore be able to extrapolate the displacement back in time from the observed value using the observed growth rate. Looking 1 ms before the observed instability gives a displacement

$$\xi = (1\ cm)\exp -\left(\frac{1ms}{25\mu s}\right)$$

$$\sim 10^{-17} cm \quad .$$

This shows that the observed instability, even at its smallest amplitude has no connection with conventional linear theory. To say that the behaviour is non-linear does not, of course, contribute to our understanding. We need a new theoretical framework to deal with fast instabilities of this sort.

A tentative model is described in reference (1). This involves the coupling of two stability boundaries as illustrated in Fig. 2. When the first stability boundary is passed, stability is maintained by some weak stabilising effect. This allows progress to the second stability boundary where the weak effect fails to provide stability. At this point the basic instability would have a fast growth rate but this has been suppressed. After passing the second stability boundary the instability then grows slowly until, at some unobservable amplitude (~ the ion Larmor radius perhaps) the weak effect is lost and transition to the fast growth of the basic instability occurs, giving the appearance of a spontaneous fast instability.

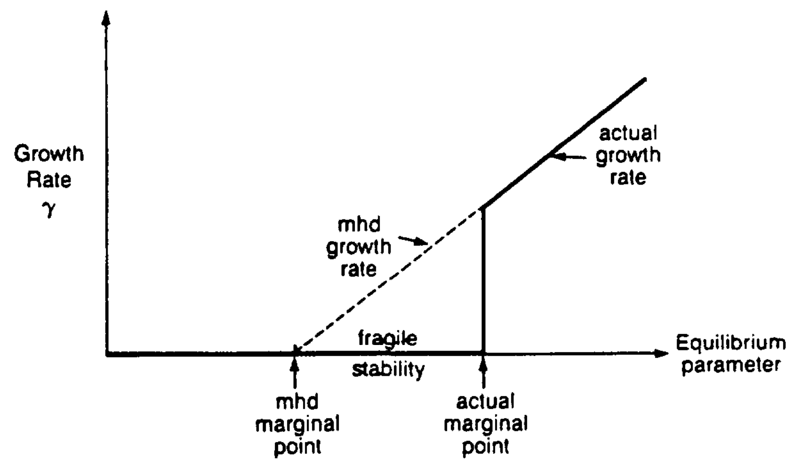

Figure 2 Illustrating a type of behaviour which would be consistent with the experimental observations. A weak stabilising effect provides a fragile stability beyond the mhd stability boundary. This allows the build up of free energy which is then suddenly released when the actual stability boundary is reached.

ii) Disruptions

Disruptions often involve a quite complex sequence of events [2]. The observed growth of mhd instabilities at the time of the disruption is a clear indication that these instabilities play a crucial role. However the principal threats posed by disruptions are related to the subsequent fast current decay which transfers current to the vacuum vessel producing very large forces, and the generation of large currents of relativistic electrons. Even the basic mhd features are more complicated than expected. In JET the form of the energy loss is not consistent with any of the theoretical models and the negative voltage spike does not appear at the expected time. These issues have been addressed in a number of papers and the present understanding is outlined below.

Figure 3 shows the behaviour of the current, temperature and loop voltage in a typical JET disruption. There has been a precursor growth of mhd instability prior to the events shown and it seems likely that the mhd perturbations are responsible for the initial fall in the temperature. However careful examination of the soft X-ray behaviour reveals a spatial structure which does not appear to be consistent with the theoretical mhd models. These models predict either multi-mode turbulence or a gross non-linear behaviour in which the m=1 and m=2 modes drive each other through profile effects. What is seen experimentally is a large modification of the soft X-ray profile, this modification having an m=1 structure. However the spatial structure of the change has the form of an "erosion" of the profile and does not correspond to the displacement expected from the theory of m=1 modes. This important issue is therefore unresolved.

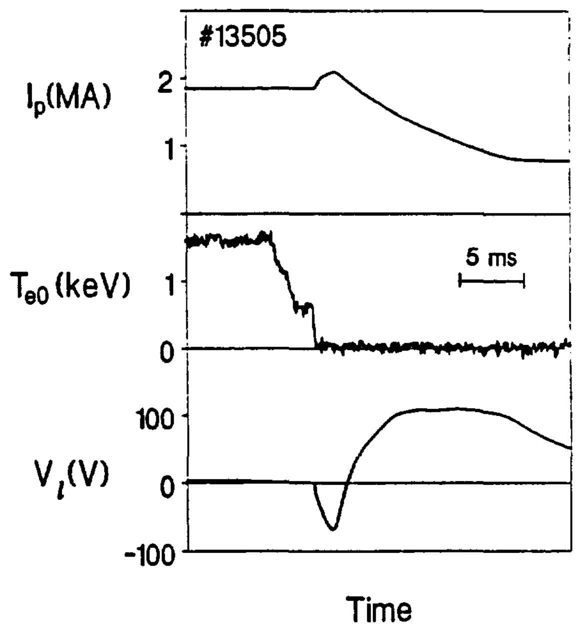

Figure 3 The temperature drop in the disruption occurs in two phases. The positive current and negative voltage spikes appear only after the second phase.

If the initial fall in temperature is due to the mhd instability then we would expect that it would also produce the observed negative voltage spike. The delay in the appearance of the spike therefore needs an explanation. A theoretical model has been developed in which the current flattening associated with the mhd instability does not extend to the plasma surface (3). This gives rise to a surrounding negative current sheet. The current configuration is frozen on the millisecond timescale because of the high electrical conductivity of the plasma. However this conductivity is suddenly reduced by orders of magnitude when the plasma temperature undergoes its second stage fall, reaching a very low temperature. The negative current then rapidly diffuses out of the plasma producing the current increase shown in figure 3 together with the associated negative voltage spike. Numerical simulations based on this model have reproduced the observed behaviour.

The final rapid fall in temperature is believed to be due to an impurity influx (4). In this model the rapid decay of the current is not due to plasma turbulence but results simply from the high resistivity of the cold plasma.

Another consequence of the increased resistivity is the production of a large current (~ MA) of runaway electrons. This arises because the critical parameter for runaway is proportional to the product, ET, of the electric field and the electron temperature. It is therefore proportional to ηjT and hence to $1/T^{1/2}$. Consequently a fall in temperature by a factor of 100 leads to an order of magnitude increase in the runaway parameter. This gives rise to a complicated runaway process which results in the observed runaway current. The velocity distribution of the electrons is unstable and calculations have been carried out to investigate the types of possible relativistic non-linear behaviour.

It is seen from the above account that disruptions can involve a complex sequence of events which have been only partly explored.

iii) Sawtooth Reconnection

It is well known that the sawtooth relaxation oscillations observed in tokamaks are not understood. In particular the Kadomtsev model appears to be in conflict with a number of experimental results. It is not clear therefore whether, or when, reconnection of the Kadomtsev type takes place. This makes it important to examine the assumptions of the model. As a result of such an examination it has been found that the assumption of resistive behaviour is seriously in question (5).

If full reconnection of the helical flux within the q=1 surface takes place on the observed timescale of the sawtooth collapse then we can calculate the resulting electric field at the reconnection layer. If we then use Ohm's law to calculate the drift-velocity of the electrons carrying the reconnection sheet current we obtain

$$v_d \sim (1-q_o)\,\frac{r_1}{R}\,\frac{\tau_e}{\tau_c}\,\omega_c\, r_1$$

Where q_o is the axial value of the safety factor, r_1 is the radius of the q=1 surface, R is the major radius, τ_e and τ_c are the electron collision time and the sawtooth collapse time and ω_c is the electron cyclotron frequency.

Using typical JET values gives $v_d \sim 3 \times 10^8$ ms^{-1} (= c). It is clear that under these circumstances the resistive model is inappropriate and that the electrons would undergo strong runaway.

A current carried by runaway electrons sees a very low resistance. However, although the electrons entering the layer rapidly acquire a large velocity in the direction of the q=1 field lines, they are immediately swept out of the layer into the magnetic island. Thus the high current density has to be maintained by the continuous acceleration of electrons entering the layer. Consequently, rather than presenting a low impedance, this form of reconnection gives a high impedance.

When electron inertia dominates, the appropriate form of Ohm's law is

$$E + v \times B = \frac{m}{ne^2} v.\nabla j \quad . \qquad (2)$$

The electric field in the layer is given by the rate, vB*, at which flux is brought in to the layer, B* being the helical magnetic field at the edge of the layer. Thus, using Ampere's law,

$$\nabla j \sim \frac{B*}{\mu_o \delta}$$

where δ is the layer thickness, equation (2) gives

$$\delta \sim \frac{c}{\omega_p} \quad , \qquad (3)$$

and the layer thickness is of the order of the collisionless skin depth.

The conventional reconnection analysis provides the expression for the reconnection time, τ, in terms of the layer thickness

$$\tau \sim \frac{r_1}{\delta} \tau_A$$

where $\tau_A = r_1 / (B^*/\sqrt{\mu_o \rho})$ and so, using relation (3), the reconnection time is

$$\tau \sim \frac{r_1 \omega_p}{c} \tau_A \quad . \qquad (4)$$

Comparing numerical predictions we find that for a typical JET sawtooth collapse having a timescale of 100 μs the prediction of Kadomtsev's model is ~ 3 ms whereas relation (4) gives ~ 300 μs. It is clear that the new model gives better agreement but there are many reservations since we do not understand the sawtooth mechanism.

Summary

From the many non-linear processes occurring in tokamaks we have chosen three quite different phenomena. Firstly, the problem of fast instabilities which is quite subtle and requires some new thinking. Secondly disruptions, which are found to be rather complex. Although explanations have been provided for some of the features, the initial energy quench does not appear to be consistent with existing theoretical models. Finally, an analysis of the Kadomtsev reconnection model leads to doubts about the applicability of the resistive Ohm's law and suggests that the effect of electron inertia would be predominant.

References

1. Wesson, J.A., Edwards, A.W. and Granetz, R.S., To appear in Nuclear Fusion (1991).

2. Wesson, J.A. et al., Nuclear Fusion 29 (1989) 641.

3. Wesson, J.A., Ward, D.J., and Rosenbuth, M.N., Nuclear Fusion 30 (1990) 1011.

4. Ward, D.J., Gill, R.D., Morgan, P.D. and Wesson, J.A., in Controlled Fusion and Plasma Heating (Proc. 15th Eur. Conf. Dubrovnick, 1988), Vol. 12B, Part I, European Physical Society (1988) 330.

5. Wesson, J.A. Nuclear Fusion 30 (1990) 2545.

APPENDIX 1.

THE JET TEAM

JET Joint Undertaking, Abingdon, Oxon, OX14 3EA, U.K.

J.M.Adams[1], F.Alladio[4], H.Altmann, R.J.Anderson, G.Appruzzese, W.Bailey, B.Balet, D.V.Bartlett, L.R.Baylor[24], K.Behringer, A.C.Bell, P.Bertoldi, E.Bertolini, V.Bhatnagar, R.J.Bickerton, A.Boileau[3], T.Bonicelli, S.J.Booth, G.Bosia, M.Botman, D.Boyd[31], H.Brelen, H.Brinkschulte, M.Brusati, T.Budd, M.Bures, T.Businaro[4], H.Buttgereit, D.Cacaut, C.Caldwell-Nichols, D.J.Campbell, P.Card, J.Carwardine, G.Celentano, P.Chabert[27], C.D.Challis, A.Cheetham, J.Christiansen, C.Christodoulopoulos, P.Chuilon, R.Claesen, S.Clement[30], J.P.Coad, P.Colestock[6], S.Conroy[13], M.Cooke, S.Cooper, J.G.Cordey, W.Core, S.Corti, A.E.Costley, G.Cottrell, M.Cox[7], P.Cripwell[13], F.Crisanti[4], D.Cross, H.de Blank[16], J.de Haas[16], L.de Kock, E.Deksnis, G.B.Denne, G.Deschamps, G.Devillars, K.J.Dietz, J.Dobbing, S.E.Dorling, P.G.Doyle, D.F.Düchs, H.Duquenoy, A.Edwards, J.Ehrenberg[14], T.Elevant[12], W.Engelhardt, S.K.Erents[7], L.G.Eriksonn[5], M.Evrard[2], H.Falter, D.Flory, M.Forrest[7], C.Froger, K.Fullard, M.Gadeberg[11], A.Galetsas, R.Galvao[8], A.Gibson, R.D.Gill, A.Gondhalekar, C.Gordon, G.Gorini, C.Gormezano, N.A.Gottardi, C.Gowers, B.J.Green, F.S.Griph, M.Gryzinski[26], R.Haange, G.Hammett[6], W.Han[9], C.J.Hancock, P.J.Harbour, N.C.Hawkes[7], P.Haynes[7], T.Hellsten, J.L.Hemmerich, R.Hemsworth, R.F.Herzog, K.Hirsch[14], J.Hoekzema, W.A.Houlberg[24], J.How, M.Huart, A.Hubbard, T.P.Hughes[32], M.Hugon, M.Huguet, J.Jacquinot, O.N.Jarvis, T.C.Jernigan[24], E.Joffrin, E.M.Jones, L.P.D.F.Jones, T.T.C.Jones, J.Källne, A.Kaye, B.E.Keen, M.Keilhacker, G.J.Kelly, A.Khare[15], S.Knowlton, A.Konstantellos, M.Kovanen[21], P.Kupschus, P.Lallia, J.R.Last, L.Lauro-Taroni, M.Laux[33], K.Lawson[7], E.Lazzaro, M.Lennholm, X.Litaudon, P.Lomas, M.Lorentz-Gottardi[2], C.Lowry, G.Magyar, D.Maisonnier, M.Malacarne, V.Marchese, P.Massmann, L.McCarthy[28], G.McCracken[7], P.Mendonca, P.Meriguet, P.Micozzi[4], S.F.Mills, P.Millward, S.L.Milora[24], A.Moissonnier, P.L.Mondino, D.Moreau[17], P.Morgan, H.Morsi[14], G.Murphy, M.F.Nave, M.Newman, L.Nickesson, P.Nielsen, P.Noll, W.Obert, D.O'Brien, J.O'Rourke, M.G.Pacco-Düchs, M.Pain, S.Papastergiou, D.Pasini[20], M.Paume[27], N.Peacock[7], D.Pearson[13], F.Pegoraro, M.Pick, S.Pitcher[7], J.Plancoulaine, J-P.Poffé, F.Porcelli, R.Prentice, T.Raimondi, J.Ramette[17], J.M.Rax[27], C.Raymond, P-H.Rebut, J.Removille, F.Rimini, D.Robinson[7], A.Rolfe, R.T.Ross, L.Rossi, G.Rupprecht[14], R.Rushton, P.Rutter, H.C.Sack, G.Sadler, N.Salmon[13], H.Salzmann[14], A.Santagiustina, D.Schissel[25], P.H.Schild, M.Schmid, G.Schmidt[6], R.L.Shaw, A.Sibley, R.Simonini, J.Sips[16], P.Smeulders, J.Snipes, S.Sommers, L.Sonnerup, K.Sonnenberg, M.Stamp, P.Stangeby[19], D.Start, C.A.Steed, D.Stork, P.E.Stott, T.E.Stringer, D.Stubberfield, T.Sugie[18], D.Summers, H.Summers[20], J.Taboda-Duarte[22], J.Tagle[30], H.Tamnen, A.Tanga, A.Taroni, C.Tebaldi[23], A.Tesini, P.R.Thomas, E.Thompson, K.Thomsen[11], P.Trevalion, M.Tschudin, B.Tubbing, K.Uchino[29], E.Usselmann, H.van der Beken, M.von Hellermann, T.Wade, C.Walker, B.A.Wallander, M.Walravens, K.Walter, D.Ward, M.L.Watkins, J.Wesson, D.H.Wheeler, J.Wilks, U.Willen[12], D.Wilson, T.Winkel, C.Woodward, M.Wykes, I.D.Young, L.Zannelli, M.Zarnstorff[6], D.Zasche[14], J.W.Zwart.

PERMANENT ADDRESS

1. UKAEA, Harwell, Oxon. UK.
2. EUR-EB Association, LPP-ERM/KMS, B-1040 Brussels, Belgium.
3. Institute National des Récherches Scientifique, Quebec, Canada.
4. ENEA-CENTRO Di Frascati, I-00044 Frascati, Roma, Italy.
5. Chalmers University of Technology, Göteborg, Sweden.
6. Princeton Plasma Physics Laboratory, New Jersey, USA.
7. UKAEA Culham Laboratory, Abingdon, Oxon. UK.
8. Plasma Physics Laboratory, Space Research Institute, Sao José dos Campos, Brazil.
9. Institute of Mathematics, University of Oxford, UK.
10. CRPP/EPFL, 21 Avenue des Bains, CH-1007 Lausanne, Switzerland.
11. Risø National Laboratory, DK-4000 Roskilde, Denmark.
12. Swedish Energy Research Commission, S-10072 Stockholm, Sweden.
13. Imperial College of Science and Technology, University of London, UK.
14. Max Planck Institut für Plasmaphysik, D-8046 Garching bei München, FRG.
15. Institute for Plasma Research, Gandhinagar Bhat Gujat, India.
16. FOM Instituut voor Plasmafysica, 3430 Be Nieuwegein, The Netherlands.
17. Commissiariat à L'Energie Atomique, F-92260 Fontenay-aux-Roses, France.
18. JAERI, Tokai Research Establishment, Tokai-Mura, Naka-Gun, Japan.
19. Institute for Aerospace Studies, University of Toronto, Downsview, Ontario, Canada.
20. University of Strathclyde, Glasgow, G4 ONG, U.K.
21. Nuclear Engineering Laboratory, Lapeenranta University, Finland.
22. JNICT, Lisboa, Portugal.
23. Department of Mathematics, Univeristy of Bologna, Italy.
24. Oak Ridge National Laboratory, Oak Ridge, Tenn., USA.
25. G.A. Technologies, San Diego, California, USA.
26. Institute for Nuclear Studies, Swierk, Poland.
27. Commissiariat à l'Energie Atomique, Cadarache, France.
28. School of Physical Sciences, Flinders University of South Australia, South Australia SO42.
29. Kyushi University, Kasagu Fukuoka, Japan.
30. Centro de Investigaciones Energeticas Medioambientales y Techalogicas, Spain.
31. University of Maryland, College Park, Maryland, USA.
32. University of Essex, Colchester, UK.
33. Akademie de Wissenschaften, Berlin, DDR.

CR 88.49.1A